Progress Towards the Second-Generation Atomic Fountain Clock at NIST

E.A. Donley, T.P. Heavner, M.O. Tataw, F. Levi*, and S.R. Jefferts
Time and Frequency Division
National Institute of Standards and Technology
Boulder, CO 80305 USA
edonley@boulder.nist.gov

***Abstract* – We present results on the performance of two important subsystems for NIST-F2 – the second-generation atomic fountain clock at NIST. Firstly, we demonstrate the efficient capture of cesium atoms from a low-velocity intense source (LVIS) of atoms into an optical molasses. Our typical LVIS flux was 10^{10} s^{-1}. The initial molasses fill rate was $R_{t=0} = 3.8(5)\times10^{9} s^{-1}$, which is consistent with 100% atom capture given the lifetime of our vacuum system. Secondly, recent results for our launch performance in the (1,1,1) fountain geometry are presented. We were able to cool the atoms to a temperature of 1.5 μK with our current design. Our plans for improving the laser cooling performance are also presented.**

Keywords-atomic beams; atomic clocks

I. INTRODUCTION

The accuracy of primary frequency standards is limited by how well one can correct for systematic frequency shifts. In the cesium atomic fountain NIST-F1, the limiting systematic uncertainties arise from corrections for the blackbody radiation shift and the spin-exchange shift. The next-generation fountain clock, NIST-F2, is being designed to reduce the size of these systematic frequency shifts so that their corrections also have reduced uncertainties [1]. Reducing the uncertainty of the spin-exchange shift is the main issue addressed here.

The primary frequency standard NIST-F1 is described in detail in [2]. In NIST-F1, one ball of atoms is launched per lineside for each clock cycle. With some minor variations in the details, this mode of operation has been the standard approach for development of atomic fountains around the world, with the notable exceptions of a juggling ^{87}Rb fountain [3] and a continuous-beam fountain that is being developed [4].

This paper describes a continuation of work on the multiple-velocity fountain concept first proposed [5] and subsequently experimentally investigated [6] by Levi and coworkers. The method effectively reduces the density of the atomic sample by nearly an order of magnitude, and reduces the size of the spin-exchange shift by a comparable factor. The total atom number is maintained, and thus the fountain stability is not significantly compromised. The idea is to launch many atom balls in rapid succession, with each ball having a fraction of the number of atoms required to reach the target stability. Atom balls launched later in the sequence have lower apogees, such that no ball ever crosses paths with any other ball during the Ramsey interrogation. All balls meet in the detection zone and are detected simultaneously, thus reducing the significance of technical noise. Calculated trajectories for such a scheme of launching 10 balls per measurement are shown in Fig. 1.

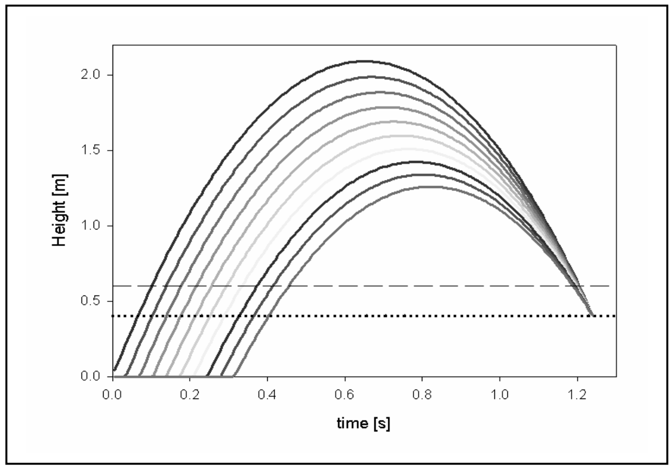

Figure 1. Calculated trajectories for a multi-toss scheme. The positions of the Ramsey cavity and the detection zone are shown as dashed and dotted lines, respectively. For this example, 10 balls of atoms were launched at 35 ms intervals. The highest trajectory has an initial velocity of 6.4 m/s.

The multiple-velocity launch method requires a high fill rate for the optical molasses. The optical molasses that was used for the initial demonstration of the multiple velocity fountain [6] was loaded from a Cs oven, which limited the fill rate to $\sim 1.6\times10^{8}\ s^{-1}$ at short times [7]. At this rate, it takes over 50 ms to load sufficient atoms to produce a sample of 10^6 state-selected atoms. We would like to load at least that many atoms in about 25 ms.

A low-velocity intense source (LVIS) of atoms [8] is a compact, high-flux, atomic beam source. A schematic drawing of an LVIS apparatus is shown in Fig. 2. The feature that distinguishes an LVIS apparatus from a standard magneto-optical trap (MOT) is the gold-coated quarter-wave plate with a hole drilled through its center that is used in place of one of the MOT beam retro-reflectors. The hole casts a shadow through the MOT, creating an imbalance in the scattering rate from the forward- and backward-traveling laser beams. This creates a net force that accelerates the cold atoms through the hole and out of the trap. An LVIS using ^{87}Rb atoms [8] typically exhibits an atomic flux of order 10^{10}/s, a tunable axial velocity of order 15 m/s with a narrow velocity spread of order 2 m/s, and transverse velocities of order 5 cm/s. LVIS studies with cesium atoms have demonstrated similar performance but with somewhat lower axial velocity (5-10 m/s), owing to the greater atomic mass of ^{133}Cs [10].

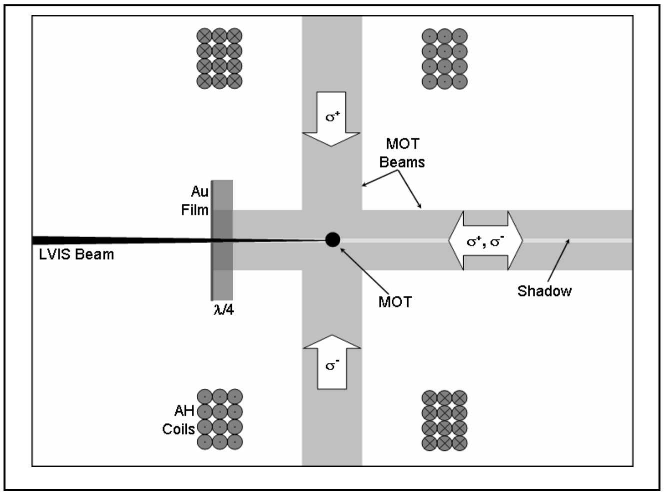

Figure 2. A schematic drawing of the LVIS apparatus. A third pair of MOT laser beams perpendicular to the plane of the figure is not shown.

With these properties, an LVIS should be an ideal source for loading atoms into an optical molasses [11]. The capture force for typical values of the laser intensity and detuning in an optical molasses is shown versus the atomic velocity v in Fig. 3. For sufficiently large detuning, the force is peaked at velocities of $v = \pm\delta / k$, where δ is the laser detuning and k is the wavevector of the laser light. The intensity of the molasses beams determines the magnitude of the force. The low velocity and narrow velocity distribution of an LVIS beam, combined with the molasses capture force versus velocity, suggest that it should be possible to achieve a capture efficiency of nearly 100 % for a beam of LVIS atoms into an optical molasses if enough laser power is available for the molasses beams.

Figure 3. Molasses capture force. The curve was calculated for a 1-D

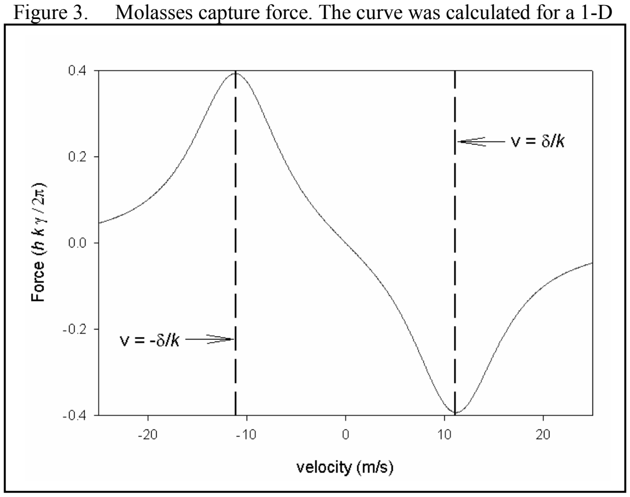

optical molasses with detuning 2.5γ and a saturation parameter $I/I_{sat} = 5$, where I_{sat} is the saturation intensity.

Our primary objective for loading the molasses from an LVIS beam is the increased load rate. A bonus for reducing the molasses loading time is a reduction in dead time of fountain operation. Even for a fountain running in the standard single-ball launch mode, reduction of the dead time between interrogations improves the stability directly by reducing the cycle time. The stability degradation arising from the Dick effect [12] is also minimized by reducing the dead time.

Another advantage of loading a molasses from an LVIS is the tremendous gain in differential pumping. The thermal cesium source in an LVIS is far from the sensitive part of the vacuum system where background collisions are to be avoided, and the vacuum system can even be designed such that the MOT chamber is connected to the fountain vacuum system only through the 0.5 mm diameter hole in the LVIS mirror through which the LVIS beam emerges.

To avoid light shifts in the fountain, running in the multiple-velocity fountain mode necessitates rotating the orientation of the molasses beams such that none of the beams travels along the axis of the toss tube. This is accomplished in the (1,1,1) launch geometry. If the six faces of a cube represent the planes orthogonal to each molasses beam, in the (1,1,1) geometry the cube is oriented such that it stands symmetrically with respect to gravity on a single point and the toss tube axis is along the diagonal of the cube. The molasses beams in this geometry are at angles of $\pm 37.3^\circ$ with respect to the molasses midplane.

An added bonus for operating in the (1,1,1) geometry is that this configuration removes the need for a window at the top of the toss tube. Not having a window near the apogee of the fountain will simplify the evaluation of the blackbody radiation shift. The reduction of the blackbody shift is another focus for the development of NIST-F2 and will be discussed in future publications.

II. APPARATUS

A. LVIS

Details on our LVIS experiments can also be found in [13]. A gold-coated quarter-wave plate of 5 cm diameter and with a hole of 0.5 mm diameter drilled through its center served as one of the MOT retroreflectors, and was mounted inside of the vacuum chamber in a custom 70 mm 6-way cube cross at the right end of the apparatus, as shown in Fig. 4. To accommodate this custom optic in the vacuum chamber, a 114 mm conflat flange was welded flush against one of the cube faces. To maximize the MOT load rate, the MOT trapping beams had a diameter of 2.5 cm ($1/e^2$). This required the use of large-diameter (5 cm) polarizing optics. There were no magnetic-field trim coils on the MOT chamber. The anti-Helmholz coils were mounted to an x,y,z translation stage, and the entire coils were moved to locate the trap center with respect to the shadow cast by the hole.

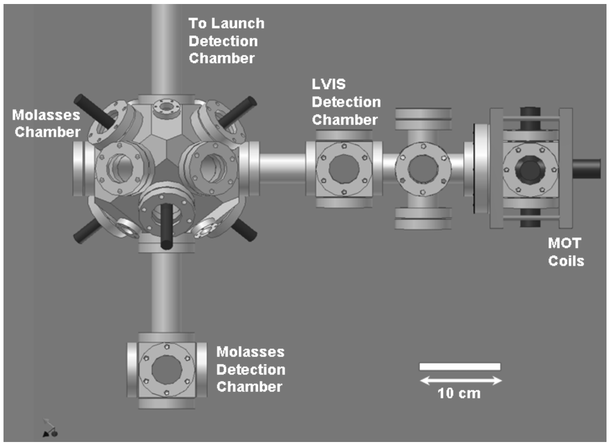

Figure 4. The apparatus. For simplicity, the molasses and MOT beams are shown as cylinders protruding through the vacuum flanges. The scale is indicated by the 10 cm bar on the lower right.

The atomic beam emerging through the hole in the gold-coated waveplate was measured and optimized in the LVIS detection chamber located 22 cm downstream from the MOT. A standing-wave light sheet that was 1 mm thick and tuned to the $|F=4\rangle \rightarrow |F'=5\rangle$ cycling transition served as the detection beam. Repump light tuned to the $|F=3\rangle \rightarrow |F'=4\rangle$ transition was overlapped with the detection light. The fluorescence was collected on a photodiode with a collection efficiency of 1.5×10^{-3} and amplified. This signal was fed to a lock-in amplifier. The fluorescence signal was modulated by chopping the repump light with a shutter. When the LVIS flux was maximized, it was possible to see the LVIS fluorescence from the detection beam with an infrared viewer, but lock-in detection was needed for optimization.

Laser light red-detuned from the $|F=4\rangle \rightarrow |F'=5\rangle$ cycling transition was provided to the molasses through three fiber collimators that produced 1.0 cm diameter ($1/e^2$) beams. These adjustable collimators were mounted to the chamber on the studs that also attached the windows to the chamber. Those beams were retro-reflected through quarter-wave plates to produce a lin $\perp$ lin polarization arrangement. For the LVIS measurements, atoms were not launched upward, but rather they were dropped and detected 25 cm below the center of the molasses chamber. The atoms fell through a standing-wave light sheet that was 1 mm thick and resonant with the cycling transition, and their fluorescence was focused by a compound lens onto a photodiode with a high-gain amplifier.

The molasses detection system was calibrated as follows. The molasses was loaded for 400 ms, the molasses beams were turned off, and the atoms fell through the light sheet in the detection zone. A 1 mm^2 aperture was placed directly in the front of the center of the collection lenses. Photons that clear this aperture travel through the lenses and onto the 1 cm^2 photodiode at near-normal incidence, and were assumed to be detected with 100 % efficiency. 100 atom balls were allowed to fall through the detection system and their signals were averaged. The peak voltage corresponding to the solid angle of the aperture was determined. This measurement gave a calibration factor of 350 volts/steradian. The aperture was then removed, and the voltage for the full aperture (1 cm^2) of the detection system was measured. This voltage was divided by the calibration factor to arrive at a collection efficiency of 1.3×10^{-3}. The number of atoms loaded into the molasses was double-checked with two calibrated CCD cameras that imaged the molasses directly, and the results were consistent with both detection methods.

B. (1,1,1) Launch Apparatus and Procedure

For the (1,1,1) launch measurements, a fixed 6-collimator design was implemented. For NIST-F2, the launch chamber will be surrounded by magnetic shields, which will make optics adjustment difficult. We designed the molasses chamber and fiber collimators to achieve precise optical alignment without adjustment. The molasses chamber was designed to have flat outside faces orthogonal to the axis of each molasses beam. The collimators were located off these flat faces and were centered on the window flanges. The collimators were pre-aligned on the bench before mounting to the vacuum chamber. The beam diameter was 13 mm ($1/e^2$). The beam pointing errors were as large as 1 mrad.

The laser light for the molasses beams was provided with two double-pass acousto-optic modulators–one for the up beams and one for the down beams. The light from each double pass was divided into three beams with two half-wave plates and two polarizing beam splitters. The light was then injected into optical fibers for delivery to the beam collimators.

The launch sequence that led to the lowest atom temperatures for a launch height of 1 m was as follows. Atoms were collected in an optical molasses for 300 to 500 ms. The molasses beams were then turned off and the atoms were allowed to fall for 25 ms. We expect that allowing the atoms to fall briefly before launch improves the effectiveness of the post-cool by extending the time that the atoms are in the molasses region[14]. Then the atoms were launched in a moving molasses by turning the molasses beams back on with the frequency of the up (down) beams shifted from the initial molasses frequency by +3 MHz (-3MHz) for 2 ms. Finally, the atoms were cooled in the moving frame with a post-cool sequence by ramping the frequency of the molasses beams by 46 MHz to the red of the launch frequency and to zero intensity in 1 ms. The atoms were detected 41 cm above the optical molasses with a standing wave light sheet tuned to the cycling transition. Fluorescence from the atoms was collected with a photodiode and amplified. For our (1,1,1) launch experiments we did not use our LVIS to load the molasses, but rather the atoms were loaded from a cesium oven.

III. LVIS MEASUREMENTS

A. Flux

The typical LVIS flux was 10^{10} atoms/s. The optics did not require extensive realignment from day to day as long as the anti-Helmholz MOT coils were allowed to heat up completely, since thermal drifts were significant.

The required MOT field gradient was typical for a large MOT. The anti-Helmholz coils were coaxial with the LVIS beam such that the LVIS beam escaped the MOT along the strong axis of the trap. The LVIS flux began to saturate when the field gradient along the strong (weak) axis was 7(3.5) gauss/cm. The total power required for the MOT laser-beams was 100 mW.

One difference between our study and those performed previously [8,10] is that we observe the peak flux at a detuning of about 2γ, whereas Lu et al. [8] observed the peak flux for ^{87}Rb atoms at a detuning of over 5γ, where γ is the linewidth of the optical transition. Their flux versus detuning curve was also about 4 times broader than what we observed. Wang and Buell [10] also observed a very broad flux versus detuning curve, and like us, they studied ^{133}Cs atoms. One difference between our measurements and these previous studies is that our LVIS beam escaped on the strong axis of our trap, whereas their LVIS beam escaped along one of the two weak axes. This affects how quickly the LVIS atoms are Zeeman-shifted out of resonance on their way out of the trap. In our experiment, the atoms are shifted out of resonance twice as fast. This experimental detail could make our LVIS beam less sensitive to deflection from intensity imbalances in the MOT beams.

The laser detuning that maximizes the number of trapped atoms in a MOT is 3.2γ. We suspect that the reason that our flux was peaked closer to resonance is that the vacuum on the MOT side of the LVIS mirror could have been as high as 10^{-7} torr for our experiment. A detuning closer to resonance results in a LVIS beam of higher velocity [8], and thus the atoms spend less time in the region that has a higher collision rate. We did not measure the velocity of the LVIS beam directly, but in the next section, we infer the beam velocity based on the characterization of the optical molasses.

B. Optical Molasses Capture

The molasses fill rate was very sensitive to the molasses detuning, the optimum value of which was 2.5γ. The simulation of the 1-D molasses capture force shown in Fig. 2 is based on the optimal molasses parameters. Based on the modeled capture force and the measured detuning sensitivity of the fill rate, one can deduce that the velocity of the LVIS beam was ~11 m/s, which is consistent with the measurements of Wang and Buell [10] for our experimental parameters. The total number of molasses atoms saturated at an intensity corresponding to $5I_{sat}$. A higher intensity was required when the alignment of the molasses beams was not optimized.

The number of molasses atoms, N, measured as a function of load time is shown in Fig. 5. The fill curve was fit to $N = a\left(1-e^{-t/\tau}\right)$. The data fit to $a = 1.1(1)\times10^{9}$ atoms and τ = 290(30) ms. The fill rate at short times gives the relevant fill rate of $R_{t=0} = a/\tau = 3.8\times10^{9}\ s^{-1}$. At this rate, it would require 26 ms to capture 10^8 atoms. This loading rate is over two orders of magnitude larger than the loading rate for the optical molasses on our atomic fountain NIST-F1, which is loaded from a cesium oven.

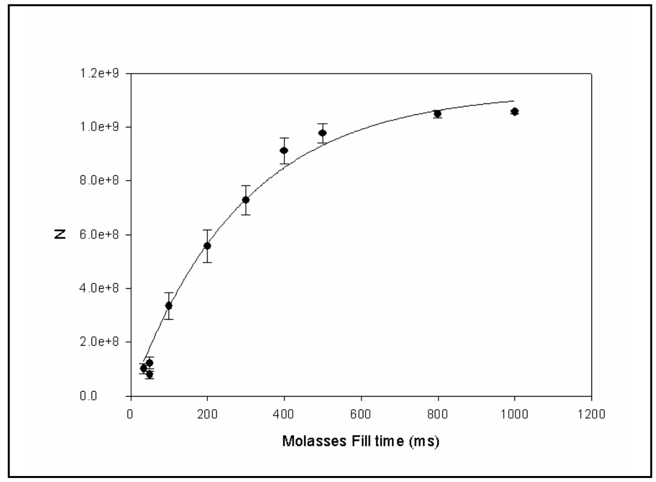

Figure 5. Number of atoms captured in the optical molasses versus fill time. The y-axis has been calibrated with camera data. The error bars are errors estimated from other measurements, but each individual point represents a single measurement. The error bars represent statistical uncertainties alone–calibration errors of the detection system could be larger, but are the same for all measurements.

The lifetime of the atoms in the molasses is 310(20) ms. The decay time constant was measured by starting with a full molasses and then turning off the repump light to the MOT, which extinguishes the LVIS beam. The molasses was then held for some time before the number of remaining molasses atoms was measured. The observed lifetime is consistent with a background gas pressure of 3×10^{-8} torr, which agrees with the pressure we find based on the current readings on the ion pump controllers (a few microamperes). This relatively high pressure for this system is understood and is the result of leaks caused by damage during transport of the apparatus.

Assuming the molasses decay arises from background collisions, if there were no background collisions the fill rate would be two times higher than what we have observed. Thus the level of agreement between the molasses capture rate and the total LVIS flux is within the calibration uncertainties(50 %) of the LVIS detection system, and our capture rate is consistent with capturing 100 % of the LVIS atoms in the optical molasses.

C. Implied Stability

The stability of an atomic fountain as a function of the total measurement time τ is expressed in terms of the Allan deviation $\sigma_y(\tau)$ as

$$\sigma_y(\tau) = \frac{1}{\pi Q_{at}}\sqrt{\frac{T_c}{N_d \tau}} \qquad (1)$$

Q_{at} is the frequency of the hyperfine transition divided by the width of the central Ramsey fringe, T_c is the cycle time (a full cycle consists of tossing two atom balls), and N_d is the number of detected atoms. Our LVIS apparatus can load 10^7 state-selected atoms in 25 ms. Assuming a 20 % return fraction (which we achieve in the fountain NIST-F1), $Q_{at} = 1\times10^{10}$, and $T_c = 1.8$ s, this would imply a stability of $\sigma_y(\tau) = 3\times10^{-14}\tau^{-1/2}$. Launching as many as 10 atom balls per line side could bring the short-term stability down to the $1\times10^{-14}\tau^{-1/2}$ level. In practice, the stability would be limited by that of the local oscillator, which has a stability of 8×10^{-14} at 1.8 s (Oscilloquartz 8607-BM)[15]. If we used a local oscillator with a higher short-term stability (such as a cryogenic oscillator, for example), local comparisons could be made between the fountain and another local clock at the $1\times10^{-14}/\sqrt{\tau}$ level.

IV. (1,1,1) GEOMETRY LAUNCH

Most of the launch measurements were performed for a launch height of 1.0 m. To measure the temperature, the atom spatial distribution was measured in the detection zone for balls of atoms on their way up and on their way down. The atom velocity distribution was then found via a deconvolution procedure. For all of the data that we collected, similar results for the velocity distribution were found by simply assuming Gaussian distributions for the initial ball size and velocity spread. The lowest temperature that we have achieved thus far is 1.5 μK, which corresponds to an atom velocity of 0.95 cm/s. We did not observe a temperature dependence on launch height.

V. NEAR TERM IMPROVEMENTS

1.5 μK is significantly warmer than the 0.5 μK that we are able to achieve in NIST-F1, and would correspond to a reduction of a factor of 2 in the NIST-F1 atom throughput. We attribute the inferior laser-cooling performance to two factors: imperfect molasses beam pointing and insufficient molasses beam intensity control. The level of accuracy of the beam pointing for our current design was 1 mrad. For the next round of experiments, we will modify the collimator design to allow for two-dimensional translation of the fiber output with respect to the lens axes to correct for pointing errors. To improve our level of control of the molasses beam intensities, we will build a double-pass acousto-optic modulator system for each molasses beam. This will make it possible to control the intensity of each beam independently and will also make it simple to eventually servo-control the intensity of the beams.

ACKNOWLEDGMENTS

The authors thank E. Cornell for the use of the custom LVIS mirror and J. Shirley and S. Knappe for valuable comments on this manuscript.

REFERENCES

[1] S.R. Jefferts, T.P. Heavner, E.A. Donley, J.H. Shirley, and T.E. Parker, "Second generation cesium fountain primary frequency standards at NIST," 2003 IEEE IFCS, Tampa, FL, May 2003, pp. 1084.

[2] S.R. Jefferts, J.H. Shirley, T.E. Parker, T.P. Heavner, D.M. Meekhof, C.W. Nelson, F. Levi, G. Costanzo, A. DeMarchi, R.E. Drullinger, L. Hollberg, W.D. Lee, and F.L. Walls, "Accuracy evaluation of NIST-F1," *Metrologia*, vol. 39, pp. 321-336, 2002.

[3] C. Fertig and K. Gibble, "Laser-cooled ^{87}Rb Clock," *IEEE Trans. Instrum. Meas.*, vol. 48, pp. 520-523, 1999.

[4] G. Dudle, A. Joyet, P. Berthoud, G. Mileti, and P. Thomann, "First results with a cold cesium continuous fountain resonator," *IEEE Trans. Instrum. Meas.*, vol. 50, pp. 510-514, 2001.

[5] F. Levi, A. Godone, and L. Lorini, "Reduction of the cold collisions frequency shift in a multiple velocity fountain: a new proposal," *IEEE Trans. Ultrason., Ferroelect., Freq. Contr.*, vol. 48, pp. 847-850, 2001.

[6] F. Levi, A. Godone, L. Lorini, S.R. Jefferts, T.P. Heavner, and C. Calosso, "The multiple velocity fountain: a new scheme for the cold collision frequency shift reduction," *Proc. 2001 Freq. Stand. Metrology Symp.*, pp. 466-468, 2001.

[7] T.P. Heavner, L. Hollberg, S.R. Jefferts, J. Kitching, W. Kipstein, D.M. Meekhof, and H.G. Robinson, "Characterization of a cold cesium source for PARCS: Primary atomic reference clock in space," *IEEE Trans. on Instrumentation and Measurement* vol. 50, pp. 500-502, 2001.

[8] Z.T. Lu, K.L. Corwin, M.J. Renn, M.H. Anderson, E.A. Cornell, and C.E. Wieman, "Low-velocity intense source of atoms from a magneto-optical trap," *Phys. Rev. Lett.* 77, pp. 3331-3334, 1996.

[9] C.Y. Park, M.S. Jun, and D. Cho. "Magneto-optical trap loaded from a low-velocity intense source," J. Opt. Soc. Am. B. vol. 16, pp. 994-997, 1999.

[10] H. Wang and W.F. Buell, "Velocity-tunable magneto-optical-trap-based cold Cs atomic beam," JOSA B. 20, pp. 2025-2030, 2003.

[11] H.J. Metcalf and P. van der Straten, *Laser Cooling and Trapping*. New York: Springer Verlag, 1999, pp. 87-97.

[12] G. Santarelli, C. Audoin, A. Makdissi, P. Laurent, G.J. Dick, and A. Clairon, "Frequency stability degradation of an oscillator slaved to a periodically interrogated atomic resonator," *IEEE Trans. Ultrason., Ferroelect., Freq. Contr.*, vol. 45, pp. 887-894, 1998.

[13] E.A. Donley, T.P. Heavner, and S.R. Jefferts, "Optical molasses loaded from a low-velocity intense source of atoms," *IEEE Trans. Instrum. Meas.,* in press.

[14] W.M. Klipstein, Jet Propulsion Laboratories, Private Communication.

[15] Products or companies named here are cited only in the interest of complete scientific description, and neither constitute nor imply endorsement by NIST or by the US government. Other products may be found to serve just as well.

* - Permanent address – Instituto Elettrotecnico Nazionale "G. Ferraris" Str. Delle Cacce 91, Torino, Italy.